Bias Correction of Zero-Inflated RCM Precipitation Fields: A Copula-Based Scheme for Both Mean and Extreme Conditions

RAJIB MAITY

Department of Civil Engineering, Indian Institute of Technology Kharagpur, Kharagpur, India, and Institute of Meteorology and Climate Research (IMK-IFU), Karlsruhe Institute of Technology, Campus Alpin, Garmisch-Partenkirchen, Germany

MAYANK SUMAN

School of Water Resources, Indian Institute of Technology Kharagpur, Kharagpur, India

PATRICK LAUX AND HARALD KUNSTMANN

Institute of Meteorology and Climate Research (IMK-IFU), Karlsruhe Institute of Technology, Campus Alpin, Garmisch-Partenkirchen, and Institute of Geography, University of Augsburg, Augsburg, Germany

(Manuscript received 13 June 2018, in final form 26 January 2019)

ABSTRACT

Changes in extreme precipitation due to climate change often require the application of methods to bias correct simulated atmospheric fields, including extremes. Most existing bias correction techniques (i) only focus on the bias in the mean value or on the extreme values separately, and (ii) exclude zero values from analysis, even though their presence is significant in daily precipitation. We developed a copula-based bias correction scheme that is suitable for zero-inflated daily precipitation data to correct the bias in mean as well as in extreme precipitation at any specific statistical quantile. In considering the whole of Germany as a test bed, the proposed scheme is found to work well across the entire study area, including the German Alpine regions. The joint distribution between observed and regional climate model (RCM)-derived precipitation is developed through copulas. In particular, the joint distribution is modified to make it discrete at zero in order to account for zero values. The benefit of considering zero precipitation values is revealed through the improved performance of bias correction both in the mean and extreme values. Second, the quantile that best captures the bias (whether in the mean or any extreme value) is determined for a specific location and varies spatially and seasonally. This relaxation in selecting the location-specific optimal quantile renders the proposed methodology spatially transferable. By acknowledging possible changes in extreme precipitation due to climate change, the proposed scheme is expected to be suitable for climate change impact assessments for extreme events worldwide.

1. Introduction

The systematic under or overestimation of hydroclimatic variables by any climate model is known as bias, and may be contingent on geographical and climatological factors as well as the specific choice of the climate model (Christensen et al. 2008; Maraun et al. 2010; Hagemann et al. 2011; Mao et al. 2015; Maraun et al. 2017). In spite of some recent advancements, simulated climate variables are often found to have significant biases (Wilby et al. 2000; Christensen et al. 2008; Teutschbein and Seibert 2010; Jang and Kavvas 2013). For example, many regional climate models (RCMs) generate excessive numbers of wet days with light rainfall (also known as the drizzle effect), underestimate heavy rainfall values, and/or produce incorrect seasonal variations in rainfall (Schmidli et al. 2006; Fowler et al. 2007; Christensen et al. 2008;

Supplemental information related to this paper is available at the Journals Online website: https://doi.org/10.1175/JHM-D-18-0126.s1.

Corresponding author: Rajib Maity, rajib@civil.iitkgp.ac.in

DOI: 10.1175/JHM-D-18-0126.1

Teutschbein and Seibert 2010; de Elía et al. 2017; Maraun et al. 2017). The existence of bias is also recognized in statistical downscaling tools such as localized constructed analogs (LOCA) (Pierce et al. 2014) and multivariate adaptive constructed analogs (MACA) (Abatzoglou and Brown 2012). Moreover, bias in extreme values is even greater due to the higher level of uncertainty associated with these events (Nikulin et al. 2011).

Although bias correction can be a controversial topic of discussion among the scientific community (Ehret et al. 2012), the adverse effects of biases in climatological forcing data on hydrological models are widely studied (e.g., Kunstmann et al. 2004; Christensen et al. 2008; Ott et al. 2013). Therefore, before using any simulated climate variable in hydrological impact studies, bias correction is required due to the still limited performance of RCM raw output for hydrological purposes. Bias correction approaches can be categorized as either linear (Lenderink et al. 2007; Hempel et al. 2013), nonlinear (Leander and Buishand 2007; Leander et al. 2008; Hempel et al. 2013), or empirical- or distribution-based quantile mapping (Wood et al. 2004; Block et al. 2009; Michelangeli et al. 2009; Li et al. 2010; Piani et al. 2010; Dosio and Paruolo 2011; Johnson and Sharma 2011; Thrasher et al. 2012; Mao et al. 2015; Pierce et al. 2015). Reviews of the different bias correction methods can be found in the literature (Teutschbein and Seibert 2010; Lafon et al. 2013; Pierce et al. 2015; Dang et al. 2017). However, the majority of existing approaches suffer from at least one of the following shortcomings: (i) the models try to correct the bias in the mean, sometimes median and standard deviation, but not the bias in the extreme values; (ii) the models ignore the presence of zero values and consider only the nonzero values (however, the number of zero values may be significant in daily precipitation at many locations); (iii) the models are unable to preserve the shape of the probability distribution of the variable, mostly at the tail ends. A thorough discussion is presented by Pierce et al. (2015). Different types of bias correction schemes include quantile mapping (QM) (Thrasher et al. 2012), cumulative distribution function transform (CDF-t) (Michelangeli et al. 2009), equidistant quantile matching (EDCDFm) (Li et al. 2010), and an extension of EDCDFm that preserves the ratio between the model-predicted future change in mean precipitation (PresRat) (Pierce et al. 2015). A few studies focus on biases in extreme values separately (Rojas et al. 2011; Cai et al. 2013; Jeon et al. 2016). However, consideration of the entire range of the variable is necessary to provide a complete (stochastic) representation of the association between downscaled and observed values that in turn helps to correct the bias in extremes values, where relevant. Moreover, the use of a joint probability distribution between the observed and simulated climate variable may lead to better results. Hence, we propose a stochastic copula-based bias correction scheme that is able to take care of the aforementioned issues in correcting biases in extreme values, besides the mean bias of zero-inflated daily precipitation. The performance of the proposed bias correction scheme is compared with another copula-based methodology that does not consider zero values in precipitation [i.e., without zero values (WZV)] (Mao et al. 2015). The proposed method is additionally compared with QM as another popular bias correction method.

Copulas are statistical tools used to model the dependence between two or more random variables in order to develop a joint distribution between them (Nelsen 2006). Multivariate studies involving copulas in hydrology include the analysis of droughts (e.g., Laux et al. 2009; Madadgar and Moradkhani 2013; Zhang et al. 2013; Borgomeo et al. 2015), rainfall (Maity and Nagesh Kumar 2008), evaluation of the modeling of the spatial dependence of rainfall by regional climate models (Hobaek Haff et al. 2015), downscaling of rainfall (van den Berg et al. 2011; Ben Alaya et al. 2014; Lorenz et al. 2018), soil moisture prediction (Das and Maity 2015; Pal et al. 2017), streamflow prediction in ungauged catchments (Samaniego et al. 2010), floods (Sraj et al. 2015), and catchment compatibility studies (Grimaldi et al. 2016). Copula-based models are also used for the bias correction of RCM output (Laux et al. 2011; Mao et al. 2015). However, these studies have considered only nonzero pairs while ignoring other possible combinations, that is, zero observed value and nonzero simulated downscaled value, nonzero observed value and zero simulated downscaled value, or both being zero (Mao et al. 2015). The assumption of ignoring zero values in either observed or simulated downscaled values can be accepted only if their number is small. However, the presence of such cases is often significant for variables like daily precipitation. Thus, consideration of zero values is essential for accurate bias correction. Here lies the motivation of the present study.

2. Methodology

The methodology utilizes copulas to capture bivariate association between observed (OBS) and simulated downscaled values (SDV). However, the existence of significant zero values in both OBS and SDV leads to a mixed marginal distribution with a probability mass at zero values. Therefore, in order to study the dependence structure between OBS and SDV, the pairs are divided into three groups: (i) pairs where both OBS and SDV are nonzero positive values, (ii) pairs where OBS = 0, and (iii) pairs where SDV = 0. Using these groups, three sets of information are extracted from the categorized pairs as part of the model's development. These are (i) parameters for the best-fit copula model for the pairs where both OBS and SDV are nonzero positive values, (ii) a suitable decay function capturing the probability of zero OBS, conditioned on SDV over its entire range, and (iii) conditional probability distribution of OBS values when SDV = 0. Furthermore, by combining this information, a set of simulation curves for the conditional probability distribution of OBS values given any value of SDV is obtained, which is used to obtain bias-corrected precipitation [hereafter bias-corrected values (BCV)].

a. Model for nonzero positive SDV

The model for nonzero positive SDV uses two sets of information: (i) parameters of the best-fit copula model for the pairs where both OBS and SDV are nonzero and (ii) a suitable decay function capturing the probability of zero OBS, conditioned on SDV over its entire range.

1) BEST-FIT BIVARIATE COPULA MODEL FOR NONZERO POSITIVE PAIRS OF SDV AND OBS

The bivariate association between positive pairs of SDV and OBS is captured by fitting an appropriate bivariate copula function. To fit a copula function, the variables are converted to their reduced variate using appropriate marginal distributions. The best-fit marginal distributions are determined for both associated random variables, that is, precipitation values from nonzero pairs of OBS and SDV. In this study, a total of 12 parametric probability distributions (beta, exponential, gamma, generalized pareto, inverse Gaussian, logistic, log logistic, lognormal, normal, Rayleigh, Rician, and Weibull) are fitted to the nonzero pairs of OBS and SDV individually, and the best-fit distribution is selected as the marginal distribution for the respective variable. The selection of the best-fit marginal distribution is based on two criteria: (i) the fitted marginal distribution should pass the chi-square (χ^2) test at the 95% significance level, and (ii) it should have the lowest Bayesian information criterion (BIC) (Schwarz 1978; Wit et al. 2012). If no probability distribution is found to fulfill both criteria, then a nonparametric Gaussian kernel-based estimate of probability distribution (hereafter nonparametric distribution) is selected as the marginal distribution. The OBS and SDV are transformed to their respective reduced variate (nonexceedance probability), that is, $F_{X_1}(x_1)$ and $F_{X_2}(x_2)$.

Copula functions can be utilized to model the dependence between random variables as they are able to estimate the joint probability distribution using the reduced variate of the random variables. According to Sklar's theorem, the joint distribution between random variables X_1 and X_2 [$F_{X_1,X_2}(x_1, x_2)$] is expressed as (Nelsen 2006; Maity 2018):

$$F_{X_1,X_2}(x_1,x_2) = C\left[F_{X_1}(x_1), F_{X_2}(x_2)\right], \tag{1}$$

where C is the bivariate copula function and $F_{X_i}(x_i)$ ($i = 1, 2$) are the marginal distributions of the random variable X_i. There are different theoretical bivariate copula functions, and the best-fit copula is selected. The conditional distribution of any one of the random variables (say X_1) can be expressed as (Joe 1996):

$$F_{X_1/X_2}(x_1|x_2) = \frac{\partial C\left[F_{X_1}(x_1), F_{X_2}(x_2)\right]}{\partial F_{X_2}(x_2)}. \tag{2}$$

In the above expressions, an appropriate copula function C is required to model the dependence between nonzero pairs of OBS and SDV. Different copula functions exist to model different kinds of dependence (Nelsen 2006; Schmidt 2007; Mao et al. 2015). In this study, four copula functions (namely Clayton, Gumbel, Gaussian, and Frank) are used. Two of the most popular statistics used to select the most appropriate (best fit) copula are Kolmogorov–Smirnov (T_n) and Cramér–von Mises (S_n). The T_n statistics measure the absolute distance between the empirical copula C_n, obtained directly from data and a parametric copula function C_θ (Genest et al. 2009; Das and Maity 2015). The empirical copula function C_n is defined by

$$C_n(u,v) = \frac{1}{n}\sum_{i=1}^{n}[(U_i \le u) \wedge (V_i \le v)], \quad 0 \le u, v \le 1, \tag{3}$$

where n is the number of data points, $U_i = F_{X_1}(x_{1i})$ and $V_i = F_{X_2}(x_{2i})$. The terms x_{1i} and x_{2i} are the ith value from series X_1 and X_2, respectively. The symbol "$\wedge$" indicates the logical "and", that is, the occurrence of both arguments. The Kolmogorov–Smirnov statistic (T_n) is defined as

$$T_n = \max|\sqrt{n}[C_n(u,v) - C_\theta(u,v)]|. \tag{4a}$$

The Cramér–von Mises statistic (S_n) is the sum of the square of the difference between the empirical and fitted copula, that is,

$$S_n = \sum_{i=1}^{n} [C_n(u,v) - C_\theta(u,v)]^2, \tag{4b}$$

where C_n and C_θ are as explained before. Lower values of these statistics indicate a better fit. In the case of a conflict, importance is given to S_n as its power is higher than T_n (Genest et al. 2009). Thus, the copula function showing the lowest value of these statistics is selected as the best-fit copula function to model the dependence.

Following the selection of the best-fit copula function, the conditional probability distribution of OBS conditioned on SDV is computed using Eq. (2), considering OBS as X_1 and SDV as X_2. Next, the obtained conditional distribution needs to be modified considering the possibility of zero precipitation, conditioned on SDV, which is explained in the following section.

2) Probability of no precipitation (zero OBS) conditioned on SDV

The second group of data, that is, pairs where OBS = 0, is used to calculate the probability of OBS being zero given some value of SDV. First, the entire range of SDV is divided into a number of classes (bins) and the frequency of the corresponding OBS being zero in these classes is calculated. These probabilities are expected to decrease with increasing values of SDV. Thus, an exponential decay curve is used to model this probability of no observed precipitation (zero OBS) as a function of the SDV value. The function is in the form of

$$Y = ae^{bX}, \tag{5}$$

where Y is the probability of no precipitation (zero OBS) and X is the value of SDV. The parameters a and b are estimated by a least squares error approach during model calibration from the second group of data, considering X as the mean of the upper and lower bound of the respective class of SDV, and Y as the computed probability of no precipitation for different classes. It is obvious that the negative values of b will indicate *decay* and goodness-of-fit can be assessed through the coefficient of determination r^2.

This fitted curve is used to compute the probability of zero precipitation for a given value of SDV. The computed probability is taken as the probability mass for zero BCV at the given SDV and is used to update the conditional probability distribution obtained from the copula. This is carried out as follows: knowing a specific value of SDV, the probability of zero precipitation is obtained from the fitted curve (say p). Assigning this value of p as the probability mass for zero precipitation, the rest of the conditional probability distribution of BCV is updated (Maity 2018). The updated conditional probability distribution of BCV, $\tilde{F}_{X_1/X_2}(x_1|x_2)$, is expressed as

$$\tilde{F}_{X_1/X_2}(x_1|x_2) = \begin{cases} p, & \text{for} \quad x_1 = 0, x_2 > 0 \\ p + (1-p)F_{X_1/X_2}(x_1|x_2), & \text{for} \quad x_1 > 0, x_2 > 0 \end{cases}, \tag{6}$$

where $F_{X_1/X_2}(x_1|x_2)$ is obtained from Eq. (2) considering C as the most appropriate copula selected as explained in the previous section and p is as defined before. Thus, the updated conditional probability distribution becomes a mixed distribution. A schematic representation of this modification of conditional distribution is shown in Fig. 1. Henceforth, the updated conditional probability distribution of BCV is simply referred to as the conditional probability distribution of BCV. It is noted that the conditional probability distribution is valid for nonzero SDV only. The case of zero SDV is explained in the following section.

b. Model for zero SDV

For this part of the model, the final group of data (pairs where SDV = 0) is used. With these data, the frequencies of no precipitation (zero OBS) are computed and a suitable probability distribution for the nonzero OBS is ascertained, resulting in a mixed distribution having a probability mass at zero OBS. Thus, the form of final distribution is similar to Eq. (6) (but with different parameters) and is expressed as

$$F_{X_1/X_2=0}(x) = \begin{cases} M, & \text{for} \quad x_1 = 0, x_2 = 0 \\ M + (1-M)G_X(x), & \text{for} \quad x_1 > 0, x_2 = 0 \end{cases}, \tag{7}$$

where M is the frequency of zero OBS, determined from the y intercept of the fitted curve for probability of no precipitation [$Y = ae^{bX}$, explained in section 2a(2)] and $G_X(x)$ is the distribution for nonzero OBS for the pairs where SDV = 0. Therefore, M is eventually equal to parameter a in Eq. (5), and the method to ascertain $G_X(x)$ is the same as that for the marginal distribution, explained in section 2a(1).

It is noted that these two parts of the model result in a complete set of probability simulation curves for the entire range of SDV, including zero. Finally, Eqs. (2), (5), (6), and (7) provide complete information for different

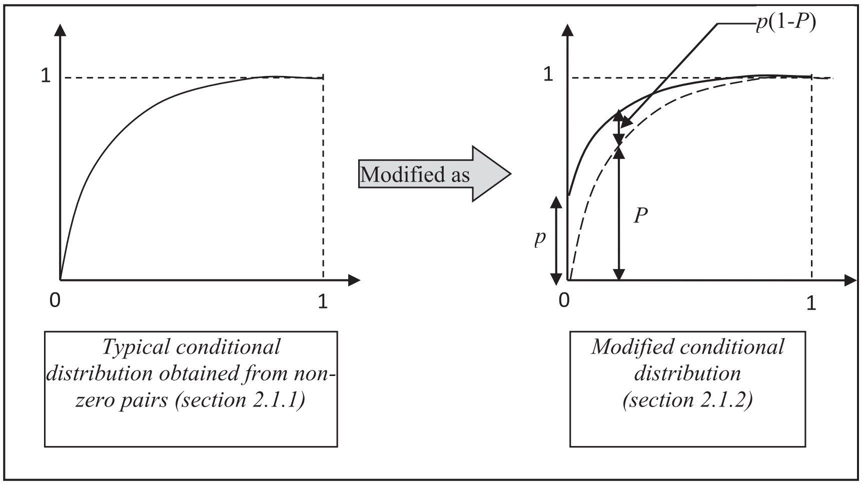

FIG. 1. Schematic representation of modifying the conditional distribution to accommodate the occurrence of zero values in observed precipitation. The modified value, i.e., $P + p(1 - P)$, is rearranged as $p + P(1 - p)$ and presented in Eq. (5).

combinations including zero values and can hence be used for bias correction for any desired quantile values.

The obtained conditional distribution varies spatially and the probability mass at zero also varies owing to its geographical location and climatology. Consequently, the quantile that best represents the observed value for a particular percentile including extremes needs to be ascertained at each location. The optimal quantile is a parameter of the model that varies with location and the target percentile of the observed precipitation. For example, which quantile of the conditional distribution (derived from the copula) best corresponds to the 50th quantile, that is, the median of the observed precipitation? Or which quantile of the conditional distribution (derived from the copula) best corresponds to the 95th quantile of the observed precipitation (extreme values)? It varies over space and is thus location specific. It needs to be determined from the historical data during model calibration. Estimation of the optimal quantile is straightforward because it is based on minimizing the mean absolute distance between observed and bias-corrected values. In other words, the quantile that yields the lowest mean absolute deviation (AD_{mean}, discussed in the subsequent section) between the observed values and BCV is considered as the optimal quantile. The optimal quantile for BCV at any desired statistics is ascertained during the calibration period and tested during the validation period.

c. *Model performance evaluation*

To evaluate the model performance, the level of correspondence between SDV and BCV is assessed. Monthwise statistics (mean and extreme values) are obtained from daily SDV and BCV, and the Pearson correlation coefficient r, degree of agreement D_r, unbiased root-mean-square error (uRMSE), and mean absolute distance (AD_{mean}) are used to assess their correspondence. The statistics are obtained by pooling all of the data from each month separately and computing the statistics across the months of the study periods. It should be noted that climate model outputs cannot be time-tagged, thus monthwise statistics are extracted to evaluate the model performance at a monthly or seasonal scale. The Pearson correlation coefficient r is a measure of linear association (if any) between variables; better model performance is indicated by higher values of r. The deviation between BCV and OBS against the deviation between OBS and its mean is compared by the degree of agreement D_r, and may range between -1 and 1 (Willmott et al. 2012; Maity et al. 2016). For the best possible model, the D_r is 1. The uRMSE is the root-mean-square error calculated between the deviations of OBS and BCV from their respective means. The AD_{mean} is the mean of absolute deviations between OBS and BCV. Lower values of uRMSE and AD_{mean} indicate better model performance. Further mathematical details of these performance statistics are provided in section 1 of the online supplemental material.

3. Study area and data

The proposed bias correction scheme is applied to daily precipitation across Germany from 1971 to 2000. Regionalisierte Niederschlagshöhen (REGNIE) data, obtained from the German Weather Service (DWD), are used as the observed gridded precipitation data product. These data are available from 1951 to the present for approximately 2000 DWD observation stations. The station values are transferred to gridded values by spatial interpolation (inverse distance weighting) of the anomalies (compared to long-term means of each grid cell). For the long-term climatological mean field, a multilinear regression approach is applied, considering the geographical position, elevation, and wind exposure of the stations. The REGNIE data are available at a 1-km resolution but are upscaled in this study to match the resolution of the regional climate data. More detailed information about the dataset and the interpolation technique applied is provided in DWD (2011).

Downscaled regional climate information across Germany at high resolution constitutes a product of the regional climate model named the Weather Research and Forecasting (WRF) Model using the Advanced Research version of WRF core (WRF-ARW) (Skamarock et al. 2008). The model is forced by ERA-40 reanalysis data (Uppala et al. 2005) for the period 1971–2000. A double-nesting strategy is used to downscale the ERA-40 to a horizontal resolution of 49 km and 7 km, respectively, using 40 vertical levels. Further details about the WRF setup, the physics parameterization options applied and its biases can be found in Berg et al. (2013).

To maintain spatial homogeneity, the REGNIE data are upscaled to a 49-km horizontal resolution onto the WRF grid in such a way that the total amount of precipitation is conserved. Henceforth, the REGNIE data are referred to as OBS (or simply observed precipitation) and the WRF-ARW output is referred to as SDV (or simply RCM). The data are divided into two equal periods, 1971–85 and 1986–2000, for model calibration and validation, respectively.

4. Results and discussion

The OBS data are found to possess a few unusual values that are more than the mean plus 5 times the standard deviation. These are not extreme events and may have resulted from the existence of erroneous records in the observed data. Such outliers and their corresponding SDVs are removed from the model development. The model calibration is carried out separately for different seasons to account for the seasonal climatology. Four different seasons are chosen, that is, spring (March–May), summer (June–August), autumn (September–November), and winter (December–February). The model is run over the whole of Germany and bias-corrected precipitation fields are produced. In addition, four specific locations (marked as A, B, C, and D) are selected on the basis of different mean bias characteristics during the calibration period in order to discuss the model performance. These locations are shown in Fig. S1 in the supplemental material. Location A (grid center 51.52°N, 12.92°E) shows a significant mean wet bias throughout the year. The bias is very small at location B (grid center 51.08°N, 14.24°E) throughout the year. Location C (grid center 49.32°N, 11.60°E) and location D (grid center 49.32°N, 8.08°E) show variations between dry and wet bias during different seasons of the year. Apart from the entire bias-corrected precipitation fields, the results at these four locations will assist in discussing the model performance for all possible bias characteristics.

As described in the methodology, three sets of information are extracted from the data during the calibration period for each season at a particular location: (i) parameters for the best-fit copula model for the pairs where both OBS and SDV are nonzero positive values, (ii) a suitable decay function capturing the probability of zero OBS, conditioned on SDV over its entire range, and (iii) the conditional probability distribution of OBS values when SDV = 0.

As discussed in section 2a(1), 12 different parametric distributions are used to estimate the marginal distribution. If no parametric probability function is deemed suitable, a nonparametric probability density function is fitted over the data. It is found that the best-fitting probability distribution for OBS across the study area belongs to only four distributions, that is, exponential, generalized pareto, lognormal, and nonparametric. Similarly, for SDV, the best-fitting probability distribution belongs to only five different distributions, that is, exponential, generalized pareto, lognormal, logistic, and nonparametric. Next, the best copula function is determined at each grid point over the study area and across different seasons, as discussed in section 2a(1). The grid-wise spatial variations of the best-fit probability distribution functions and copula functions for different seasons are shown in Figs. S2 and S3, respectively, in the supplemental material. The Gaussian copula is found to be the most suitable over most regions. From the best-fit copula, the conditional distributions of precipitation, conditioned on positive SDV only, are obtained at each location and for each season.

As explained in the methodology, the conditional distribution is modified to accommodate the probability of zero precipitation. Therefore, the parameters of the exponential decay function showing the probability of no precipitation corresponding to some SDV is estimated. A typical example (location D during the winter season) is shown in Fig. 2a to fit an exponential decay curve that can be used to compute the probability

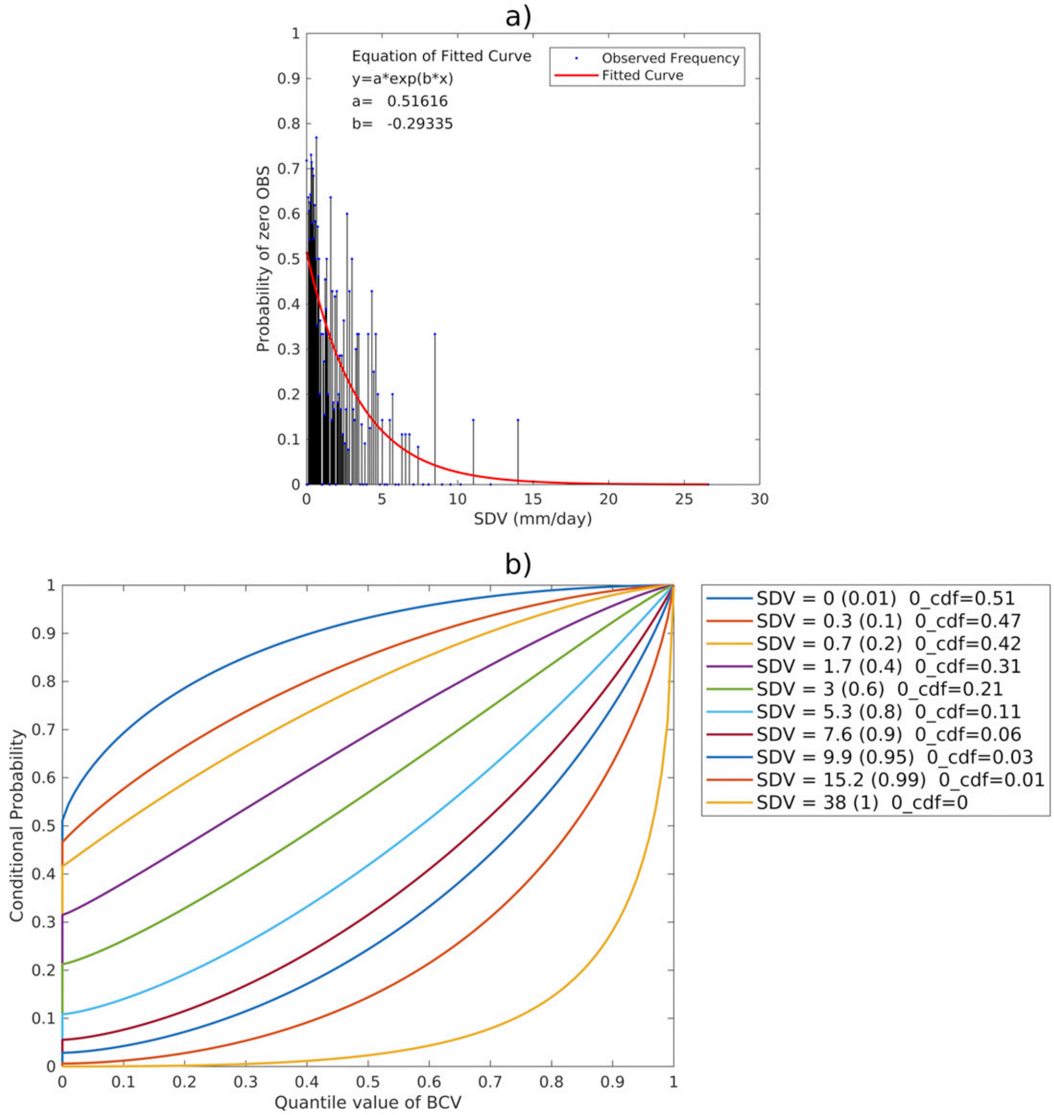

FIG. 2. (a) A typical example of fitting an exponential decay curve to compute the probability of observed precipitation being zero for a specific SDV over the entire range of SDV; (b) conditional CDF obtained from the fitted copula function and exponential decay curve for zero precipitation. In the legend, ''0_cdf'' refers to the probability mass for zero OBS, or in other words, the probability of no observed precipitation corresponding to a specific SDV (quantile value mentioned in parentheses). The conditional CDF can be generated for any specific SDV (quantile values) and 10 such typical conditional CDFs are shown in the figure. This example (both panels) is for location D (Fig. S1 in the supplemental material) in the winter.

of observed precipitation being zero for a specific SDV over the entire range of SDV. It is noticed that the frequency of no precipitation (zero OBS) decreases with increased values of SDV. A typical fitted curve with estimated parameters showing the probability of no precipitation conditioned on SDV over its entire range for location D during the winter season is also shown in Fig. 2a. Such fitted curves are used to calculate the probability of no precipitation corresponding to some value of SDV. This information is used as p in Eq. (6) (when SDV is a nonzero positive number) and as M in Eq. (7) (when SDV is zero). A typical set of modified conditional distribution curves is shown in Fig. 2b at location D during the winter season for different values of SDV. These conditional distributions are used to debias precipitation at any desired quantile. The analysis is carried out at all grid points across the study region for different seasons. Hence, four sets of calibrated models (one corresponding to each season) are obtained for each grid point.

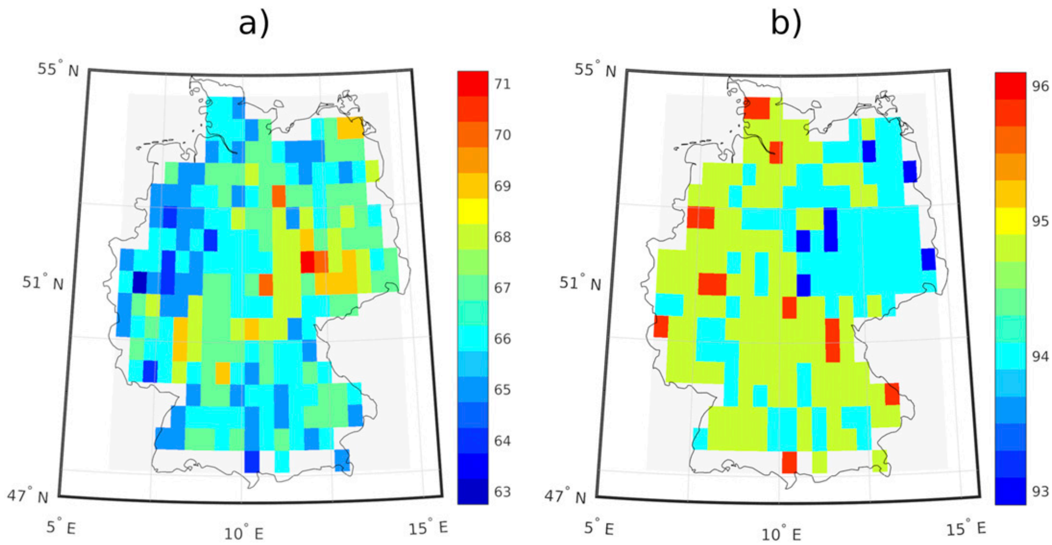

FIG. 3. Variation of optimal quantile for best correction of bias in (a) monthly mean precipitation and (b) the 95th percentile (used as a typical example of extreme magnitude) of monthly precipitation.

To obtain the optimal quantile at a particular location, BCVs are estimated from the final conditional distribution for different quantiles during the calibration period. The optimal quantile for the best correction of bias in the mean is found to vary from one location to another, within the range of 63rd and 71st across the study region (Fig. 3a). It is generally higher on the eastern than the western side.

The variation in the monthwise mean of BCV, SDV, and OBS precipitation during the calibration and validation periods at different locations (A, B, C, and D) is shown in Fig. S4 in the supplemental material, and the corresponding association measures are shown in Table 1. It can be noticed that the proposed bias correction approach is successful in reducing the mean bias of SDV precipitation at all locations. Even when the type (dry or wet) and magnitude of the bias during the validation period differ from the calibration period (e.g., locations A and D; Fig. S4b), the proposed method is found to be successful in correcting such biases, too. However, at these locations, model performance is slightly poorer but still better than SDV, with BCV being closer to OBS for most months. Table 1 also demonstrates that the error measures uRMSE and AD_{mean}

TABLE 1. Correspondence of monthwise mean of SDV and mean of bias-corrected precipitation through BCV (proposed) and existing methods (WZV and QM) with observed values. Figure S4 in the supplemental material may be used for visual comparison.

		Calibration period performance				Validation period performance			
Location	Precipitation values	r	D_r	uRMSE	AD_{mean}	r	D_r	uRMSE	AD_{mean}
A	SDV	0.52	−0.37	0.35	0.62	0.37	0.06	0.40	0.45
	BCV	0.85	0.69	0.14	0.12	0.63	0.36	0.23	0.31
	WZV	0.44	0.37	0.24	0.25	0.25	0.11	0.32	0.43
	QM	0.77	0.54	0.23	0.18	0.46	0.34	0.31	0.32
B	SDV	0.62	0.58	0.34	0.28	0.49	0.32	0.41	0.50
	BCV	0.59	0.59	0.33	0.26	0.69	0.52	0.33	0.36
	WZV	0.58	0.22	0.33	0.51	0.54	−0.05	0.37	0.78
	QM	0.77	0.62	0.29	0.25	0.64	0.46	0.35	0.40
C	SDV	0.72	0.50	0.38	0.36	0.52	0.19	0.47	0.63
	BCV	0.90	0.75	0.20	0.18	0.77	0.62	0.33	0.30
	WZV	0.87	0.49	0.22	0.36	0.45	0.16	0.45	0.66
	QM	0.88	0.73	0.24	0.20	0.57	0.40	0.45	0.47
D	SDV	0.54	0.24	0.40	0.52	0.38	−0.34	0.41	0.91
	BCV	0.78	0.68	0.23	0.22	0.70	0.43	0.30	0.34
	WZV	0.87	0.07	0.18	0.63	0.68	−0.39	0.30	0.97
	QM	0.80	0.73	0.28	0.18	0.79	0.20	0.28	0.48

are lower in BCV than in SDV. Moreover, the r and D_r are higher for BCV compared to SDV. During the validation period, the association measures are slightly poorer than for the calibration period. Moreover, in some cases, the level of correspondence between SDV and OBS during the calibration and validation periods is found to vary (e.g., locations A and D), whereas BCV is found to exhibit a considerable improvement in correspondence with OBS during both periods, indicating the efficacy of the proposed bias correction scheme. The proposed bias correction method is trained seasonally and parameters are calibrated for different locations separately; this perhaps helps in better capturing the regional and seasonal behavior of the bias.

Analysis is undertaken across the study area for each calendar month of the year. The spatial variation in monthly mean BCV for a few selected months, that is, February, May, August, and November (one month from each season) along with the corresponding monthly mean of SDV and OBS during the calibration and validation periods is shown in Figs. 4 and 5, respectively. It can be observed that the spatiotemporal variation in mean BCV better corresponds to that of mean OBS as compared to the SDV. This indicates that the mean bias is successfully corrected throughout Germany.

Next, the efficiency of correcting biases in extreme precipitation is investigated. The 95th percentile of observed precipitation during the calibration period is considered as an example threshold. The analysis is carried out all over the study area, and the range of the optimal quantile for best correction of bias at this extreme value is found to vary between the 93rd and 96th percentile across Germany (Fig. 3b). The range is smaller than the range of the optimal quantile for correction of the mean bias. The monthly means of the extreme BCVs are compared with the extreme OBS and SDV to evaluate the model performance. Specifically, comparison of the four locations selected and their correspondence is shown in Fig. S5 in the supplemental material. The performance statistics are shown in Table 2. It can be noticed from Fig. S5 that the extreme BCV corresponds very well with the extreme OBS, although the correspondence between extreme OBS and SDV is not good. For location D, the type of bias in the validation period differs from the calibration period and SDV is also very poor with respect to OBS, which may have resulted in the BCV not having the same seasonality as OBS. However, lower values of AD_{mean} compared to SDV suggest that the bias is reduced. It is worth noting here that any bias correction scheme cannot be regarded as a remedy for the inconsistency of RCM (WRF-ARW in this case). The bias correction methods heavily depend on the output quality of the driving climate models. If they fail to capture the relevant regional process, the results from the bias correction methods should be treated with caution (Maraun et al. 2017).

The spatial variation of the 95th percentile of OBS, SDV, and the mean of extreme BCV throughout Germany is shown in Figs. 6 and 7 for a few selected months (same as before) during the calibration and validation periods, respectively. It can be observed that the spatial variation of the monthly mean extreme BCV matches with the extreme observed precipitation condition to a greater extent than the extreme SDV, indicating the robustness of the proposed bias correction scheme.

It is further noticed that comparison between SDV and OBS indicates that the mean conditions are reproduced more effectively than for extreme cases. This indicates that WRF is simulating the mean condition better when compared to the extreme conditions. In such cases, a uniform correction factor (used in some existing bias correction methods, except QM) or transfer function for the entire range of precipitation is not expected to work satisfactorily, whereas our proposed bias correction scheme is able to reduce the bias for both the mean and extreme values simultaneously. The performance of the proposed bias correction scheme is compared with two different existing bias correction schemes as mentioned before. The first was proposed by Mao et al. (2015) and used a copula-based approach without considering zero values (WZV). The second scheme is the QM, which is another popular bias correction method. For QM, the appropriate probability distribution is fitted to OBS and SDV during the calibration period and the resulting transfer function is used for simulation during the validation period. The fitting of the probability distribution is undertaken as per section 2a(1). Hence, 12 different probability distributions are used [as listed in section 2a(1)] for fitting and the best is selected on the basis of passing the chi-square (χ^2) test at the 95% significance level and the lowest BIC. If no parametric distribution is deemed appropriate, then a nonparametric distribution is fitted. The correspondence between the monthwise mean (Table 1) and the extreme value (Table 2) of BCV (from the proposed model), WZV, and QM during the calibration and validation periods are evaluated in terms of different performance statistics. Furthermore, comparison between the BCV, WZV, and QM results are shown in Figs. S4 (for mean) and S5 (for extreme values) in the supplemental material. The spatial variation of the bias-corrected mean and extreme variables (BCV, WZV, and QM) are compared with that of OBS in Figs. S6 and S7 in the supplemental material, respectively. It is observed that BCV has the least bias compared to both QM and WZV in both the mean and extreme condition

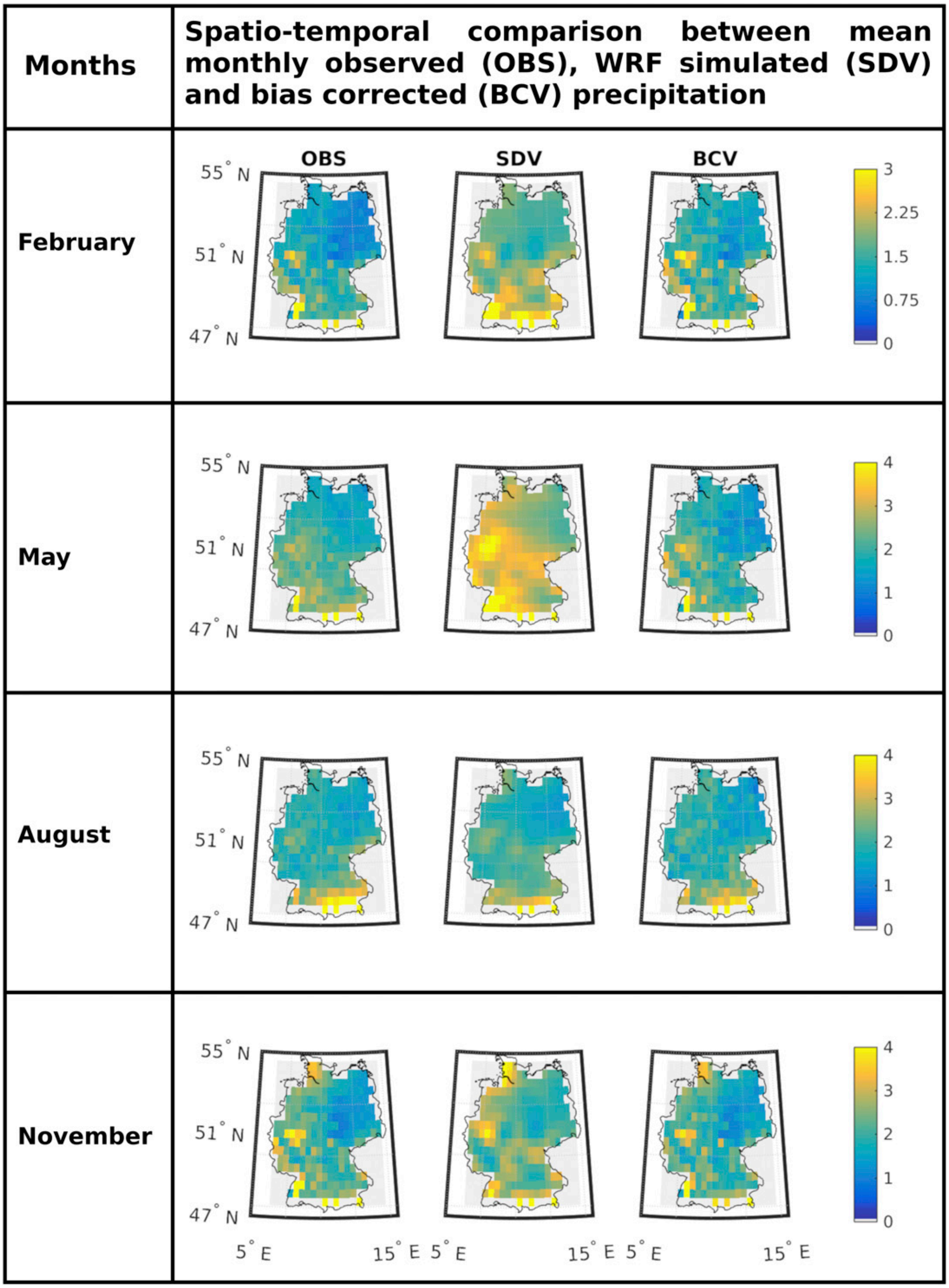

FIG. 4. Spatiotemporal comparison for mean monthly precipitation between the observed, SDV, and BCV for different months across Germany during the calibration period. Some typical months (February, May, August, and November) from different seasons are shown.

for most of the locations (Figs. S4 and S5). For instance, the values of r and D_r (0.90 and 0.75, respectively, during the calibration period and 0.77 and 0.62, respectively, during the validation period) are higher in the case of BCV than for WZV and QM (location C). At location D, QM is found to perform better than BCV for extreme values. However, the spatiotemporal distribution of BCV corresponds to OBS better than both WVZ and

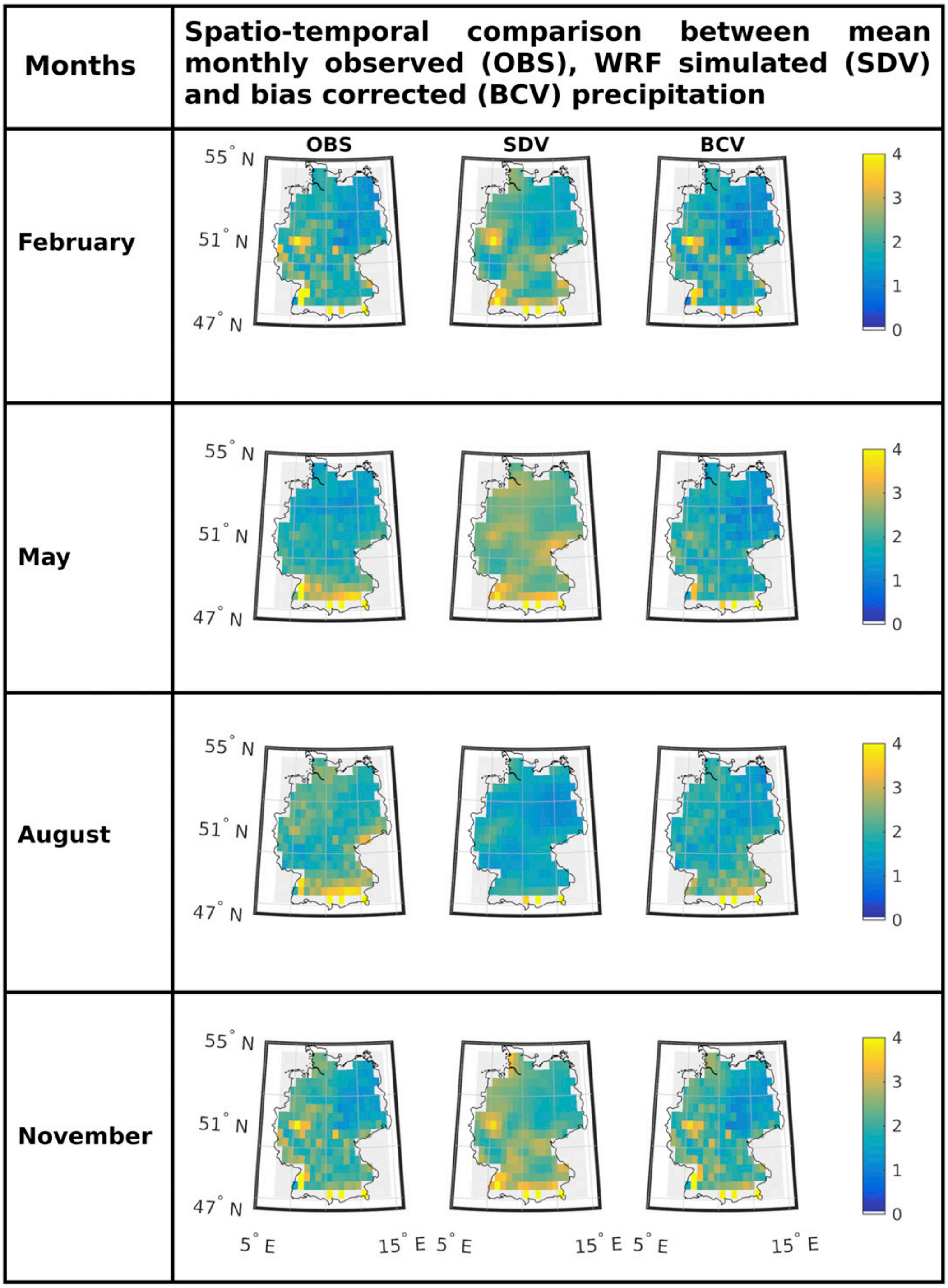

FIG. 5. As in Fig. 4, but during the validation period.

QM for the mean (Fig. S6) and extreme precipitation (Fig. S7). Among QM and WZV, WZV does not match with extreme precipitation in most cases. Overall, the results indicate the superior performance of the proposed scheme (BCV) in bias correction relative to the other two schemes. The better performance of BCV compared to WZV might owe to the fact that the proposed bias correction scheme attempts to reduce bias by considering the entire range of SDV, including the zero values, which are ignored in WZV. In the case of QM,

TABLE 2. Correspondence of monthwise extremes of SDV and bias-corrected precipitation through BCV (proposed) and existing methods (WZV and QM) with observed values (95th percentile). Figure S5 in the supplemental material may be used for visual comparison.

		Calibration period performance				Validation period performance			
Location	Precipitation values	r	D_r	uRMSE	AD_{mean}	r	D_r	uRMSE	AD_{mean}
A	SDV	0.61	0.32	1.31	1.86	0.52	0.40	1.40	1.33
	BCV	0.85	0.68	0.84	0.87	0.71	0.40	1.07	1.34
	WZV	0.09	−0.29	1.67	3.84	0.00	−0.50	1.81	4.44
	QM	0.73	0.72	1.18	0.76	0.49	0.26	1.45	1.63
B	SDV	0.56	0.37	1.88	2.18	0.59	−0.01	1.50	2.95
	BCV	0.84	0.49	1.24	1.78	0.77	0.22	1.31	2.27
	WZV	−0.15	−0.48	2.48	6.69	−0.30	−0.59	2.12	7.14
	QM	0.59	0.56	1.87	1.53	0.62	0.35	1.50	1.89
C	SDV	0.54	0.15	2.09	2.91	0.50	−0.19	2.13	3.33
	BCV	0.77	0.59	1.38	1.42	0.61	0.32	1.71	1.84
	WZV	0.03	−0.51	2.31	7.00	−0.05	−0.61	2.24	6.85
	QM	0.63	0.50	1.77	1.70	0.39	0.16	2.43	2.27
D	SDV	0.21	−0.30	2.07	3.94	0.08	−0.51	2.17	5.62
	BCV	0.25	0.48	1.77	1.44	0.04	0.16	2.18	2.30
	WZV	0.50	−0.64	1.53	7.63	0.69	−0.70	1.35	9.03
	QM	0.74	0.55	1.35	1.26	0.75	0.09	1.49	2.49

the bias is corrected by comparing the cumulative distributions of SDV and OBS. The QM assumes a fixed relationship between the quantiles of OBS and SDV. However, this assumption of a fixed relationship may not always be valid. Mao et al. (2015) have also observed that the performance of QM is not uniform throughout Germany, and rather it strongly depends upon the rank correlation between OBS and SDV. However, the proposed model considers the conditional distribution of OBS, conditioned on SDV using their joint distribution. Hence, the modeled relationship is flexible depending on the rank correlation owing to varying climatology. Moreover, different (modified) conditional distributions are used for bias correction for different values of SDV, which is not possible in QM. These reasons may result in the superior performance of BCV compared to QM.

The efficacy of the proposed bias correction scheme is established for different climate regimes, different seasons, different types of bias, and for bias in the mean as well as extreme values. However, a sufficiently long dataset is required, a general drawback of any statistical approach. A high-performance computing facility is also recommended to attain a bias-corrected precipitation field over a large area at a fine resolution. Accepting these requirements, the proposed scheme is beneficial for bias corrections in simulated precipitation fields, particularly when the extremes must be considered.

5. Summary and conclusions

Inherent biases in simulated hydroclimatic variables limit their use in different climate change impact studies. A proper assessment of hydroclimatic extremes is thus essential because climate change has proven to have profound impacts on changes in extreme events. To this end, bias correction approaches, which constitute crucial aspects of climate change impact studies, must focus on biases in extreme values aside from the mean bias. Presence and types of bias are influenced by numerous factors, including climate regime, seasons, and choice of climate models, and so they may vary both spatially and across different seasons. In this study, a stochastic copula-based bias correction scheme is proposed for zero-inflated daily precipitation.

The proposed scheme is able to correct the biases in extreme values apart from the mean bias. While copula-based approaches are established as efficient for the bias correction of RCM output, zero values are generally ignored and bias in extreme values is not corrected. The proposed scheme is developed so that it can deal with zero-inflated daily precipitation, having a mixed (discrete + continuous) marginal distribution. Consequently, unlike earlier bias correction methods, the proposed method is able to debias the entire range of precipitation, including extreme values. When comparing the performance of the proposed scheme with existing approaches, the former is found to be best.

In considering different locations with different characteristics of bias, it can be seen that the RCM-simulated values may exhibit different types and magnitudes of bias during different seasons. The proposed scheme is found to correct both dry and wet bias and/or a combination of the two. Moreover, the proposed bias correction scheme is found to reduce bias in cases where

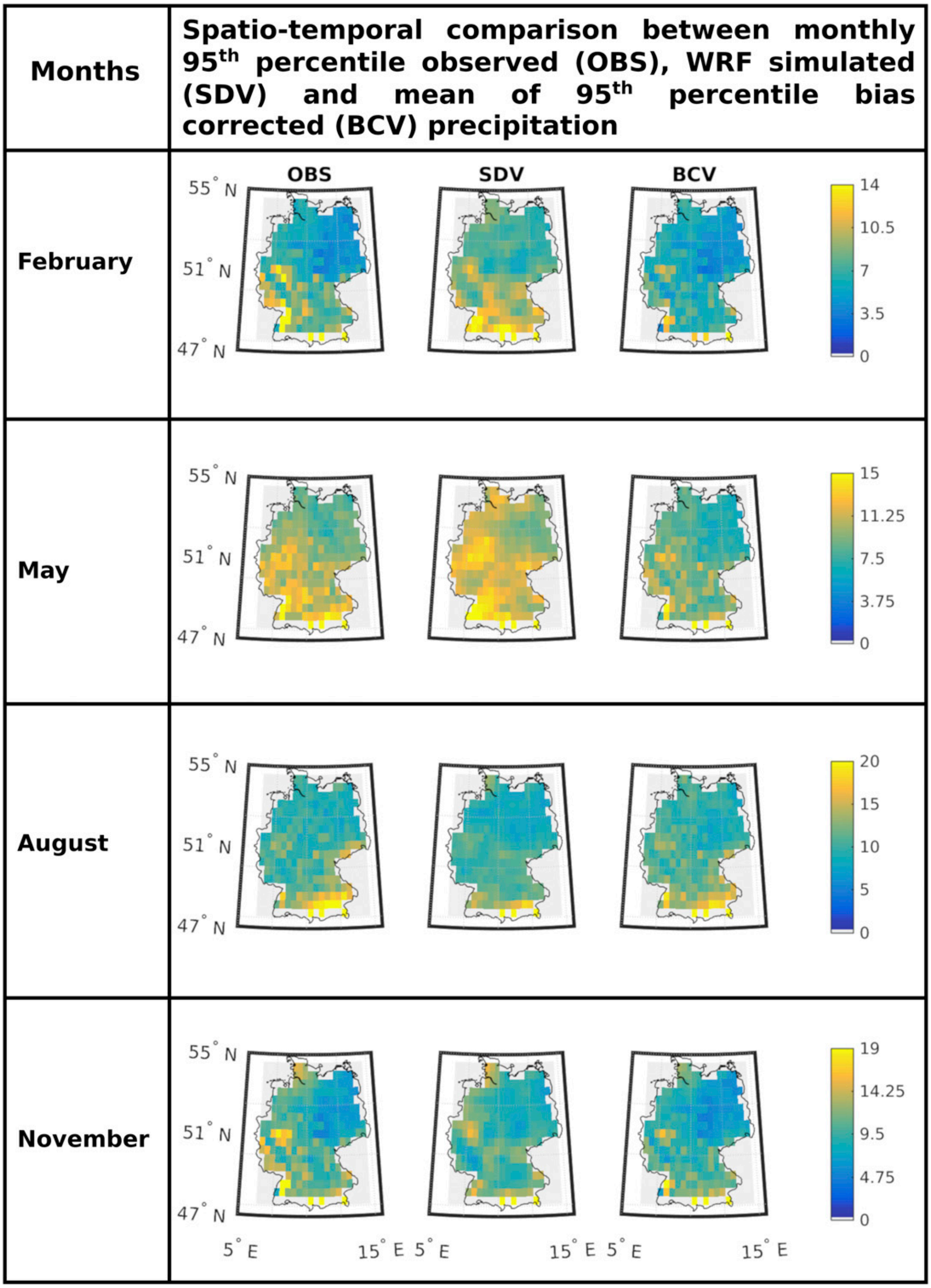

FIG. 6. Spatiotemporal comparison between the 95th percentile of observed, SDV, and BCV (extreme quartile varies with space as discussed in results) for different months across Germany during the calibration period. Some typical months (February, May, August, and November) from different seasons are shown.

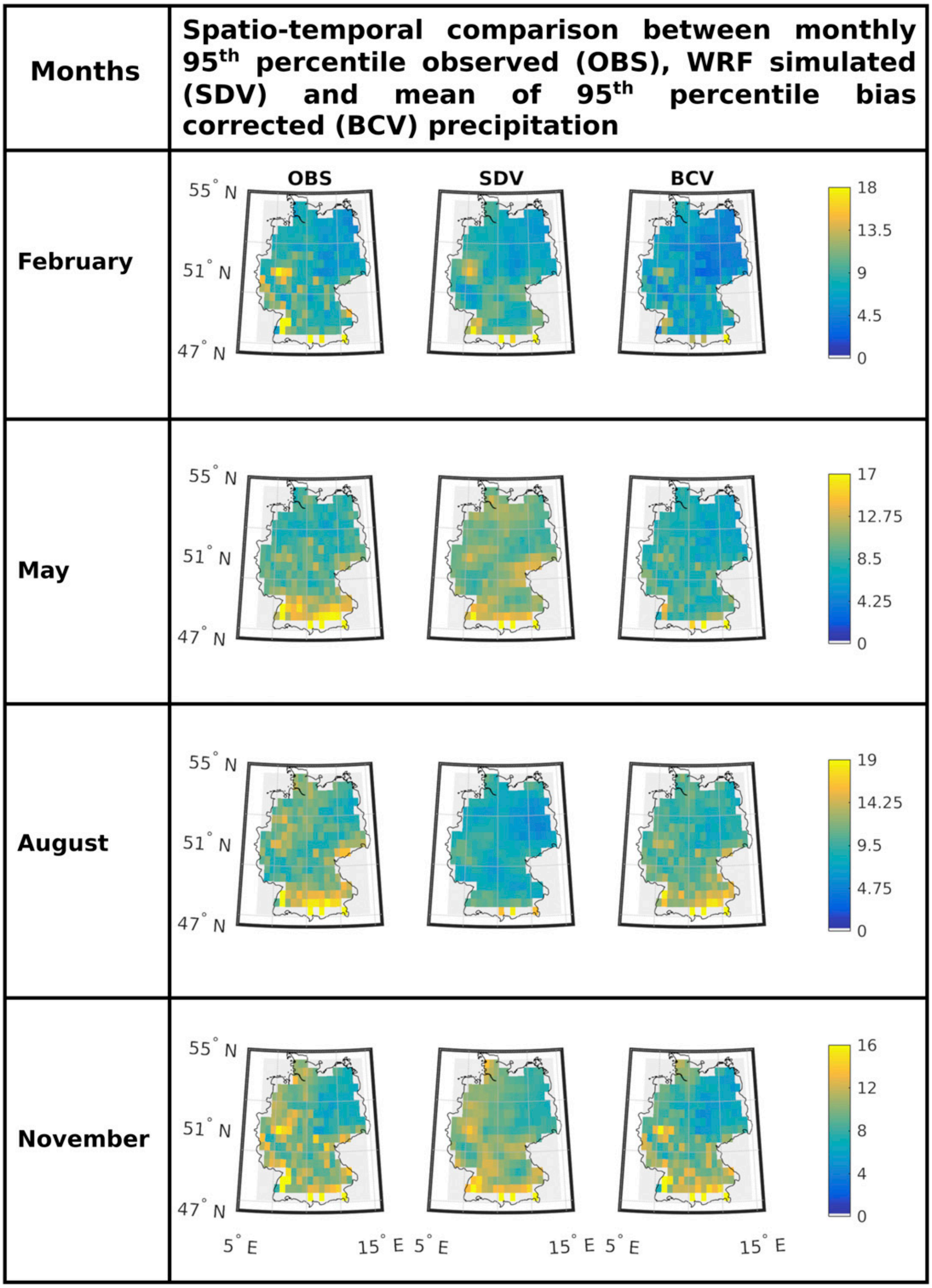

FIG. 7. As in Fig. 6, but during the validation period.

(i) the nature of the bias varies spatially between different grid points, and/or (ii) the nature of the bias varies by season at the same grid point. The optimal quantile values for the best correction of bias in mean or extreme values are found to differ across space and by season. This degree of flexibility in selecting the location-specific optimal quantile renders the proposed methodology spatially transferable. It is found to provide satisfactory debiased output all over Germany, including the German Alpine region where climatic and geographical conditions differ significantly from the rest of the country. Thus, the proposed scheme might be applicable for different locations across the world, and is expected to contribute toward the improved assessment of climate change impacts on extreme hydroclimatic events.

Acknowledgments. Corresponding author, Dr. Rajib Maity, is a recipient of the Humboldt Fellowship for Experienced Researchers from the Alexander von Humboldt Foundation, Germany. Support from the Foundation and the host institute—Karlsruhe Institute of Technology (KIT), Institute of Meteorology and Climate Research (IMK-IFU), Campus Alpin, Germany—is acknowledged. Regionalisierte Niederschlagshöhen (REGNIE) precipitation data were retrieved from the German Weather Service (DWD).

REFERENCES

Abatzoglou, J. T., and T. J. Brown, 2012: A comparison of statistical downscaling methods suited for wildfire applications. *Int. J. Climatol.*, **32**, 772–780, https://doi.org/10.1002/joc.2312.

Ben Alaya, M. A., F. Chebana, and T. B. M. J. Ouarda, 2014: Probabilistic Gaussian copula regression model for multisite and multivariable downscaling. *J. Climate*, **27**, 3331–3347, https://doi.org/10.1175/JCLI-D-13-00333.1.

Berg, P., S. Wagner, H. Kunstmann, and G. Schädler, 2013: High resolution regional climate model simulations for Germany: Part I—validation. *Climate Dyn.*, **40**, 401–414, https://doi.org/10.1007/s00382-012-1508-8.

Block, P. J., F. A. Souza Filho, L. Sun, and H.-H. Kwon, 2009: A streamflow forecasting framework using multiple climate and hydrological models. *J. Amer. Water Resour. Assoc.*, **45**, 828–843, https://doi.org/10.1111/j.1752-1688.2009.00327.x.

Borgomeo, E., G. Pflug, J. W. Hall, and S. Hochrainer-Stigler, 2015: Assessing water resource system vulnerability to unprecedented hydrological drought using copulas to characterize drought duration and deficit. *Water Resour. Res.*, **51**, 8927–8948, https://doi.org/10.1002/2015WR017324.

Cai, J. J., L. de Haan, and C. Zhou, 2013: Bias correction in extreme value statistics with index around zero. *Extremes*, **16**, 173–201, https://doi.org/10.1007/s10687-012-0158-x.

Christensen, J. H., F. Boberg, O. B. Christensen, and P. Lucas-Picher, 2008: On the need for bias correction of regional climate change projections of temperature and precipitation. *Geophys. Res. Lett.*, **35**, L20709, https://doi.org/10.1029/2008GL035694.

Dang, Q. T., P. Laux, and H. Kunstmann, 2017: Future high and low flow estimations for central Vietnam: A hydrometeorological modelling chain approach. *Hydrol. Sci. J.*, **62**, 1867–1889, https://doi.org/10.1080/02626667.2017.1353696.

Das, S. K., and R. Maity, 2015: A hydrometeorological approach for probabilistic simulation of monthly soil moisture under bare and crop land conditions. *Water Resour. Res.*, **51**, 2336–2355, https://doi.org/10.1002/2014WR016043.

de Elía, R., R. Laprise, S. Biner, and J. Merleau, 2017: Synchrony between reanalysis-driven RCM simulations and observations: Variation with time scale. *Climate Dyn.*, **48**, 2597–2610, https://doi.org/10.1007/s00382-016-3226-0.

Dosio, A., and P. Paruolo, 2011: Bias correction of the ENSEMBLES high-resolution climate change projections for use by impact models: Evaluation on the present climate. *J. Geophys. Res.*, **116**, D16106, https://doi.org/10.1029/2011JD015934.

DWD, 2011: Abteilung Hydrometeorologie: REGNIE (REGionalisierte NIEderschlage): Verfahrensbeschreibung und Nutzeranleitung. Interner Bericht im DWD, 9 pp., https://www.dwd.de/DE/leistungen/regnie/download/regnie_beschreibung_pdf.pdf.

Ehret, U., E. Zehe, V. Wulfmeyer, K. Warrach-Sagi, and J. Liebert, 2012: Should we apply bias correction to global and regional climate model data? *Hydrol. Earth Syst. Sci.*, **16**, 3391–3404, https://doi.org/10.5194/hess-16-3391-2012.

Fowler, H. J., M. Ekström, S. Blenkinsop, and A. P. Smith, 2007: Estimating change in extreme European precipitation using a multimodel ensemble. *J. Geophys. Res.*, **112**, D18104, https://doi.org/10.1029/2007JD008619.

Genest, C., B. Rémillard, and D. Beaudoin, 2009: Goodness-of-fit tests for copulas: A review and a power study. *Insur. Math. Econ.*, **44**, 199–213, https://doi.org/10.1016/j.insmatheco.2007.10.005.

Grimaldi, S., A. Petroselli, G. Salvadori, and C. De Michele, 2016: Catchment compatibility via copulas: A non-parametric study of the dependence structures of hydrological responses. *Adv. Water Resour.*, **90**, 116–133, https://doi.org/10.1016/j.advwatres.2016.02.003.

Hagemann, S., C. Chen, J. O. Haerter, J. Heinke, D. Gerten, and C. Piani, 2011: Impact of a statistical bias correction on the projected hydrological changes obtained from three GCMs and two hydrology models. *J. Hydrometeor.*, **12**, 556–578, https://doi.org/10.1175/2011JHM1336.1.

Hempel, S., K. Frieler, L. Warszawski, J. Schewe, and F. Piontek, 2013: A trend-preserving bias correction–The ISI-MIP approach. *Earth Syst. Dyn.*, **4**, 219–236, https://doi.org/10.5194/esd-4-219-2013.

Hobaek Haff, I., A. Frigessi, and D. Maraun, 2015: How well do regional climate models simulate the spatial dependence of precipitation? An application of pair-copula constructions. *J. Geophys. Res. Atmos.*, **120**, 2624–2646, https://doi.org/10.1002/2014JD022748.

Jang, S., and M. L. Kavvas, 2013: Downscaling global climate simulations to regional scales: statistical downscaling versus dynamical downscaling. *J. Hydrol. Eng.*, **20**, https://doi.org/10.1061/(ASCE)HE.1943-5584.0000939.

Jeon, S., C. J. Paciorek, and M. F. Wehner, 2016: Quantile-based bias correction and uncertainty quantification of extreme event attribution statements. *Wea. Climate Extremes*, **12**, 24–32, https://doi.org/10.1016/j.wace.2016.02.001.

Joe, H., 1996: Families of m-variate distributions with given margins and $m(m-1)/2$ bivariate dependence parameters. *Lect. Notes Monogr. Ser.*, **28**, 120–141, https://doi.org/10.1214/lnms/1215452614.

Johnson, F., and A. Sharma, 2011: Accounting for interannual variability: A comparison of options for water resources climate change impact assessments. *Water Resour. Res.*, **47**, W04508, https://doi.org/10.1029/2010WR009272.

Kunstmann, H., K. Schneider, R. Forkel, and R. Knoche, 2004: Impact analysis of climate change for an Alpine catchment using high resolution dynamic downscaling of ECHAM4 time slices. *Hydrol. Earth Syst. Sci.*, **8**, 1031–1045, https://doi.org/10.5194/hess-8-1031-2004.

Lafon, T., S. Dadson, G. Buys, and C. Prudhomme, 2013: Bias correction of daily precipitation simulated by a regional climate model: A comparison of methods. *Int. J. Climatol.*, **33**, 1367–1381, https://doi.org/10.1002/joc.3518.

Laux, P., S. Wagner, A. Wagner, J. Jacobeit, and H. Kunstmann, 2009: Modelling daily precipitation features in the Volta Basin of West Africa. *Int. J. Climatol.*, **29**, 937–954, https://doi.org/10.1002/joc.1852.

——, S. Vogl, W. Qiu, H.-R. Knoche, and H. Kunstmann, 2011: Copula-based statistical refinement of precipitation in RCM simulations over complex terrain. *Hydrol. Earth Syst. Sci.*, **15**, 2401–2419, https://doi.org/10.5194/hess-15-2401-2011.

Leander, R., and T. A. Buishand, 2007: Resampling of regional climate model output for the simulation of extreme river flows. *J. Hydrol.*, **332**, 487–496, https://doi.org/10.1016/j.jhydrol.2006.08.006.

——, ——, B. J. J. M. van den Hurk, and M. J. M. de Wit, 2008: Estimated changes in flood quantiles of the river Meuse from resampling of regional climate model output. *J. Hydrol.*, **351**, 331–343, https://doi.org/10.1016/j.jhydrol.2007.12.020.

Lenderink, G., A. Buishand, and W. van Deursen, 2007: Estimates of future discharges of the river Rhine using two scenario methodologies: Direct versus delta approach. *Hydrol. Earth Syst. Sci.*, **11**, 1145–1159, https://doi.org/10.5194/hess-11-1145-2007.

Li, H., J. Sheffield, and E. F. Wood, 2010: Bias correction of monthly precipitation and temperature fields from Intergovernmental Panel on Climate Change AR4 models using equidistant quantile matching. *J. Geophys. Res.*, **115**, D10101, https://doi.org/10.1029/2009JD012882.

Lorenz, M., J. Bliefernicht, B. Haese, and H. Kunstmann, 2018: Copula-based downscaling of daily precipitation fields. *Hydrol. Processes*, **32**, 3479–3494, https://doi.org/10.1002/hyp.13271.

Madadgar, S., and H. Moradkhani, 2013: Drought analysis under climate change using copula. *J. Hydrol. Eng.*, **18**, 746–759, https://doi.org/10.1061/(ASCE)HE.1943-5584.0000532.

Maity, R., 2018: *Statistical Methods in Hydrology and Hydroclimatology*. Springer, 444 pp., https://doi.org/10.1007/978-981-10-8779-0.

——, and D. Nagesh Kumar, 2008: Probabilistic prediction of hydroclimatic variables with nonparametric quantification of uncertainty. *J. Geophys. Res.*, **113**, D14105, https://doi.org/10.1029/2008JD009856.

——, M. Suman, and N. K. Verma, 2016: Drought prediction using a wavelet based approach to model the temporal consequences of different types of droughts. *J. Hydrol.*, **539**, 417–428, https://doi.org/10.1016/j.jhydrol.2016.05.042.

Mao, G., S. Vogl, P. Laux, S. Wagner, and H. Kunstmann, 2015: Stochastic bias correction of dynamically downscaled precipitation fields for Germany through copula-based integration of gridded observation data. *Hydrol. Earth Syst. Sci.*, **19**, 1787–1806, https://doi.org/10.5194/hess-19-1787-2015.

Maraun, D., and Coauthors, 2010: Precipitation downscaling under climate change: recent developments to bridge the gap between dynamical models and the end user. *Rev. Geophys.*, **48**, RG3003, https://doi.org/10.1029/2009RG000314.

——, and Coauthors, 2017: Towards process-informed bias correction of climate change simulations. *Nat. Climate Change*, **7**, 764–773 https://doi.org/10.1038/nclimate3418.

Michelangeli, P. A., M. Vrac, and H. Loukos, 2009: Probabilistic downscaling approaches: Application to wind cumulative distribution functions. *Geophys. Res. Lett.*, **36**, L11708, https://doi.org/10.1029/2009GL038401.

Nelsen, R. B., 2006: *An Introduction to Copulas*. 2nd ed. Springer, 218 pp., https://doi.org/10.1007/978-1-4757-3076-0.

Nikulin, G., E. Kjellström, U. L. F. Hansson, G. Strandberg, and A. Ullerstig, 2011: Evaluation and future projections of temperature, precipitation and wind extremes over Europe in an ensemble of regional climate simulations. *Tellus*, **63A**, 41–55, https://doi.org/10.1111/j.1600-0870.2010.00466.x.

Ott, I., and Coauthors, 2013: High-resolution climate change impact analysis on medium-sized river catchments in Germany: An ensemble assessment. *J. Hydrometeor.*, **14**, 1175–1193, https://doi.org/10.1175/JHM-D-12-091.1.

Pal, M., R. Maity, M. Suman, S. K. Das, P. Patel, and H. S. Srivastava, 2017: Satellite-based probabilistic assessment of soil moisture using C-band quad-polarized RISAT1 data. *IEEE Trans. Geosci. Remote Sens.*, **55**, 1351–1362, https://doi.org/10.1109/TGRS.2016.2623378.

Piani, C., J. O. Haerter, and E. Coppola, 2010: Statistical bias correction for daily precipitation in regional climate models over Europe. *Theor. Appl. Climatol.*, **99**, 187–192, https://doi.org/10.1007/s00704-009-0134-9.

Pierce, D. W., D. R. Cayan, and B. L. Thrasher, 2014: Statistical downscaling using localized constructed analogs (LOCA). *J. Hydrometeor.*, **15**, 2558–2585, https://doi.org/10.1175/JHM-D-14-0082.1.

——, ——, E. P. Maurer, J. T. Abatzoglou, and K. C. Hegewisch, 2015: Improved bias correction techniques for hydrological simulations of climate change. *J. Hydrometeor.*, **16**, 2421–2442, https://doi.org/10.1175/JHM-D-14-0236.1.

Rojas, R., L. Feyen, A. Dosio, and D. Bavera, 2011: Improving pan-European hydrological simulation of extreme events through statistical bias correction of RCM-driven climate simulations. *Hydrol. Earth Syst. Sci.*, **15**, 2599–2620, https://doi.org/10.5194/hess-15-2599-2011.

Samaniego, L., A. Bárdossy, and R. Kumar, 2010: Streamflow prediction in ungauged catchments using copula-based dissimilarity measures. *Water Resour. Res.*, **46**, W02506, https://doi.org/10.1029/2008WR007695.

Schmidli, J., C. Frei, and P. L. Vidale, 2006: Downscaling from GCM precipitation: A benchmark for dynamical and statistical downscaling methods. *Int. J. Climatol.*, **26**, 679–689, https://doi.org/10.1002/joc.1287.

Schmidt, T., 2007: Coping with copulas. *Copulas: From Theory to Application in Finance*, J. Rank, Ed., Risk Books, 3–34.

Schwarz, G., 1978: Estimating the dimension of a model. *Ann. Stat.*, **6**, 461–464, https://doi.org/10.1214/aos/1176344136.

Skamarock, W. C., and Coauthors, 2008: A description of the Advanced Research WRF version 3. NCAR Tech. Note NCAR/TN-475+STR, 113 pp., https://doi.org/10.5065/D68S4MVH.

Sraj, M., N. Bezak, and M. Brilly, 2015: Bivariate flood frequency analysis using the copula function: A case study of the Litija station on the Sava River. *Hydrol. Processes*, **29**, 225–238, https://doi.org/10.1002/hyp.10145.

Teutschbein, C., and J. Seibert, 2010: Regional climate models for hydrological impact studies at the catchment scale: A review of recent modeling strategies. *Geogr. Compass*, **4**, 834–860, https://doi.org/10.1111/j.1749-8198.2010.00357.x.

Thrasher, B., E. P. Maurer, C. McKellar, and P. B. Duffy, 2012: Technical note: Bias correcting climate model simulated daily temperature extremes with quantile mapping. *Hydrol. Earth Syst. Sci.*, **16**, 3309–3314, https://doi.org/10.5194/hess-16-3309-2012.

Uppala, S. M., and Coauthors, 2005: The ERA-40 Re-Analysis. *Quart. J. Roy. Meteor. Soc.*, **131**, 2961–3012, https://doi.org/10.1256/qj.04.176.

van den Berg, M., S. Vandenberghe, B. De Baets, and N. Verhoest, 2011: Copula-based downscaling of spatial rainfall: A proof of concept. *Hydrol. Earth Syst. Sci.*, **15**, 1445–1457, https://doi.org/10.5194/hess-15-1445-2011.

Wilby, R. L., L. E. Hay, W. J. Gutowski, R. W. Arritt, E. S. Takle, Z. Pan, G. H. Leavesley, and M. P. Clark, 2000: Hydrological responses to dynamically and statistically downscaled climate model output. *Geophys. Res. Lett.*, **27**, 1199–1202, https://doi.org/10.1029/1999GL006078.

Willmott, C. J., S. M. Robeson, and K. Matsuura, 2012: A refined index of model performance. *Int. J. Climatol.*, **32**, 2088–2094, https://doi.org/10.1002/joc.2419.

Wit, E., E. van den Heuvel, and J.-W. Romeijn, 2012: 'All models are wrong...': An introduction to model uncertainty. *Stat. Neerl.*, **66**, 217–236, https://doi.org/10.1111/j.1467-9574.2012.00530.x.

Wood, A. W., L. R. Leung, V. Sridhar, and D. P. Lettenmaier, 2004: Hydrologic implications of dynamical and statistical approaches to downscaling climate model outputs. *Climatic Change*, **62**, 189–216, https://doi.org/10.1023/B:CLIM.0000013685.99609.9e.

Zhang, Q., M. Xiao, V. P. Singh, and X. Chen, 2013: Copula-based risk evaluation of hydrological droughts in the East River basin, China. *Stochastic Environ. Res. Risk Assess.*, **27**, 1397–1406, https://doi.org/10.1007/s00477-012-0675-9.